Analysis of Beam-test data of the proposed CMS Phase II Tracker modules

A thesis submitted in partial fulfillment of the requirements for the award of the degree of

MASTER OF SCIENCE

By:
Abhishek Nag
12MS091

under
Supervisor:
Prof. Suchandra Dutta
SINP, Kolkata

Co-Supervisor:
Dr. Ananda Dasgupta
IISER Kolkata

to
Department of Physical Sciences

Indian Institute of Science Education and Research, Kolkata

April 26, 2017

Declaration

I hereby declare that this thesis is my own work and, to the best of my knowledge, it contains no materials previously published or written by any other person, or substantial proportions of material which have been accepted for the award of any other degree or diploma at IISER Kolkata or any other educational institution, except where due acknowledgement is made in the thesis. I certify that all copyrighted material incorporated into this thesis is in compliance with the Indian Copyright (Amendment) Act, 2012 and that I have received written permission from the copyright owners for my use of their work, which is beyond the scope of the law. I agree to indemnify and save harmless IISER Kolkata from any and all claims that may be asserted or that may arise from any copyright violation.

April 21, 2017
IISER Kolkata

ABHISHEK NAG
12MS091

Certificate

This is to certify that the MS thesis titled "Analysis of Beamtest data of the proposed CMS Phase II Tracker modules" submitted by Abhishek Nag, 5th year BS-MS at IISER Kolkata, is a record of bonafide research work done under my supervision. It is further certified that the thesis represents independent work by the candidate.

Prof. Suchandra Dutta
20 April, 2017

Dr. Ananda Dasgupta
20 April, 2017

Acknowledgement

I have taken efforts in this project. However, it would not have been possible without the kind support and help of many individuals and organizations. I would like to extend my sincere thanks to all of them.

I am highly indebted to Prof. Suchandra Dutta and her CMS Tracker team, comprising of Suvankar Roychowdhury and Rajarshi Bhattacharya, for their guidance and constant supervision as well as for providing necessary information regarding the project and also for their support in completing the project. The door to Prof. Dutta's office was always open whenever I ran into a trouble spot or had a question about my research or writing. She consistently allowed this paper to be my own work, but steered me in the right direction whenever she thought I needed it.

I would also like to acknowledge Dr. Ananda Dasgupta of the Department of Physical Sciences at IISER Kolkata as the Co-supervisor of this thesis, and I am gratefully indebted to him for his very valuable comments on this thesis. I also thank Dr. Ritesh Kumar Singh who motivated me and initiated the process for me to work at SINP HENPP division for my MS thesis.

I would like to express my gratitude towards my parents for their kind cooperation and encouragement which helped me in completion of this project.

And finally, last but by no means least, also to everyone in the SINP CMS group, it was great sharing time with all of you during last one year.

Thank you,
ABHISHEK NAG

Dedicated to my loving parents ...

Abstract

The silicon tracking system of the Compact Muon Solenoid (CMS) experiment at the Large Hadron Collier (LHC) at CERN needs to be replaced before the High Luminosity (HL-LHC) operation scheduled to start in 2023. A few prototype detector modules have been constructed. They were put under particle beam facility at CERN and their performance is being studied in detail. The properties that are being investigated are mainly the efficiency to detect charged particle crossing the detector, the position measurement precision etc. The performance of unirradiated detector and irradiated detector are also compared to understand the effect of the radiation damage.

Contents

List of Figures

Chapter 1

Introduction

The goal of the CMS experiment at the Large Hadron Collider (LHC) is to answer fundamental questions in particle physics. What is the origin of elementary particle masses? What is the nature of the dark matter we observe in the Universe? Are the fundamental forces unified? How does QCD behave under extreme conditions? What physics causes the dominance of matter over antimatter? In the first major physics run in 2011 and 2012, at center-of-mass energies of 7 and 8 TeV, the LHC collider reached a peak luminosity of $7.7 \times 10^{33}\text{cm}^{-2}\text{s}^{1}$, more than 75% of its design luminosity, and delivered an integrated luminosity of ≈ 25 fb^{-1} [4]. The Physics Program of the CMS experiment at the Large Hadron Collider (LHC) is off to a remarkable start! Data from CMS has yielded a vast quantity of physics results, summarized by the CMS collaboration in more than 300 publications. The highlight has been the observation in 2012 of a new particle of mass $\sim$125 GeV by the ATLAS and CMS collaborations [2, 3]. This particle was identified as a Higgs Boson.

In Run II, in 2015 and 2016, the center-of-mass energies of the CMS reached 13 TeV and delivered an integrated luminosity of ≈ 40 fb^{-1} [5].

1.1 Phase II Upgrade

The Standard Model (SM) does not provide answers to all the fundamental questions. Those require new physics. Although the 125 GeV Higgs behaves like a SM Higgs, measurement of its properties are still not very precise. Precision Higgs studies and the search for new physics and its study, when found, provide a powerful demand for higher luminosity. The LHC machine group now has a plan for achieving higher peak and integrated luminosity, well above

those for which CMS was designed. The CMS detector requires upgrades to preserve the efficiency, resolution, and background rejection of the detector at these high luminosities.

New particles are expected at the TeV scale but have not yet been seen. This could mean that they exist at masses above the current level of sensitivity. It could also mean that they could be present at lower masses but their cross sections are lower than expected or their experimental signatures are especially difficult to observe. In either case, the sensitivity for searches of new particles grows with increased luminosity.

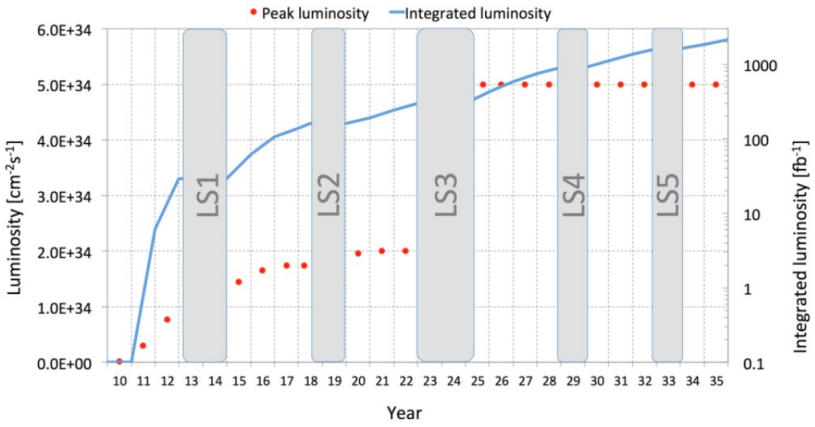

Figure 1.1: Projected LHC performance through 2035, showing preliminary dates for long shutdowns of LHC and projected luminosities

The CMS physics program at the HL-LHC will build on the experience acquired and the results obtained from more than 300 fb^{-1} of integrated luminosity accumulated in the first phase of the LHC operation. The schedule of beam operations and long shutdowns, together with projections of the peak and integrated luminosities, is shown in Figure 1.1. It can be seen that the LHC has planned to reach an integrated luminosity of 3000 fb^{-1} and increase the peak luminosity by a factor of 2.5 after Long Shutdown 3 (LS3). This phase after LS3 is called the High-Luminosity phase or Phase II of LHC and will to deliver 250 fb^{-1} per year for a further 10 years of operation.

1.1.1 Challenges of High Luminosity

The basic goal of the Phase-II upgrade is to maintain the excellent performance of the CMS detector in terms of efficiency, resolution, and background rejec-

tion for all the physics objects used in the analysis of the data. The main challenges that must be overcome to achieve this goal are radiation damage to the CMS detector from the high integrated luminosity of the HL-LHC and the very high "pileup" (PU) that comes from the high instantaneous luminosity.

For the HL-LHC, the brightness of beams and the new focusing/crossing scheme at the interaction point will enable the accelerator to potentially deliver a luminosity of 2×10^{35} $\mathrm{cm}^{-2}\mathrm{s}^{-1}$ at the beginning of each fill. This would increase the interaction rate and collision PU beyond the capabilities of existing and envisioned detector and trigger technologies. It is therefore proposed to maintain a lower, but stable instantaneous luminosity by continuously tuning the beam focus and crossing profile throughout the duration of beam fills in a process referred to as luminosity leveling. The nominal scenario is to operate at a leveled luminosity of 5×10^{34} $\mathrm{cm}^{-2}\mathrm{s}^{-1}$, corresponding to a mean pileup of 140 interactions per beam crossing. The primary goal of the Phase-II upgrade program is therefore to maintain the excellent performance of the Phase-I detector under these challenging conditions throughout the extended operation of HL-LHC.

1.2 The CMS

A schematic diagram of a general purpose detector like CMS is shown in Figure 1.2. At the heart of the experiment is a 13 m long, 6 m diameter, 4T superconducting solenoid providing large bending power for momentum measurements of charged particle. The innermost layer is a silicon-based tracker consisting of the pixel detectors followed by strip detector which give the tracking information of charged particles passing through it. Surrounding the tracker is a scintillating crystal electromagnetic calorimeter, which is itself surrounded with a sampling calorimeter for hadrons called hadronic calorimeter. Outside the magnet are the large muon detectors, which are inside the return yoke of the magnet.

1.2.1 CMS Tracker

The tracking volume is contained in a cylinder of 5.8 m length and 2.6 m in diameter. The CMS tracker is comprised of two sub-detectors with independent cooling, powering, and read-out schemes. The inner sub-detector, the pixel detector, has three layers in the barrel region. The sub-detector surrounding the pixels are the strip detector. CMS employs ten layers of silicon strip detectors,

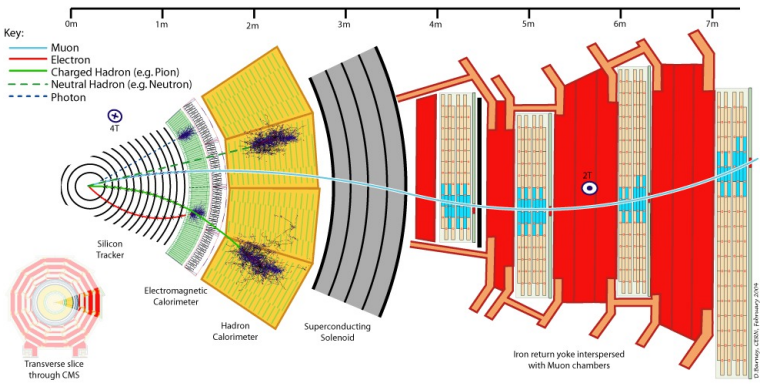

Figure 1.2: A sliced schematic representation of the CMS Detector.

which provide the required granularity and precision to reconstruct efficiently charged tracks in high multiplicity events. The silicon strip tracker with its long bending path, combined with the strong solenoidal field, provides excellent momentum resolution.

1.2.2 Limitations of the current CMS tracker

The present Outer Tracker was designed to operate without any loss of efficiency up to an integrated luminosity of 500 fb^{-1} , and an average pileup (PU) of less than 50 collisions per bunch crossing. Accumulated radiation damage in the tracker reduces the charge collection (CC)[6]. The most prominent consequence of irradiation is the increase of leakage current. The evolution of the leakage current of the tracker sensors is predicted by a detailed model that takes into account the estimated luminosity profile, the position and size of each module, the expected particle fluence at specific module locations and the expected temperature versus time scenario that includes annealing periods [7]. This model predicts that at 1000 fb^{-1} almost all the stereo modules in the barrel as well as in the endcap are no longer operational.

The loss of hits on many layers of the tracker results in a significant degradation of track reconstruction performance. The expected LHC upgrade will increase the number of interactions to the point where over-occupancy may significantly reduce track finding effectiveness. The efficiency loss decreases the physics reach of most searches for new physics, diminishes the effectiveness of high-p_T lepton isolation criteria, and degrades jet energy and missing transverse energy (MET) resolution.

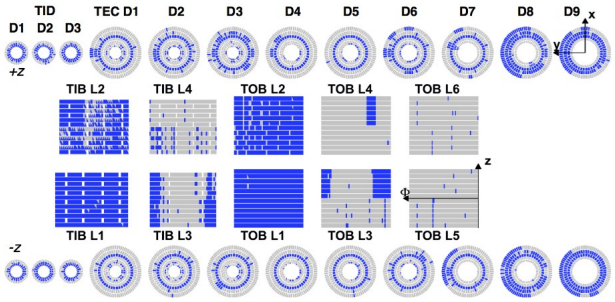

Figure 1.3: Map of non-functional modules (in blue) after an integrated luminosity of 1000 fb^{-1}, for the achievable minimum coolant temperature of -20^0C.

1.2.3 Requirements of the Tracker Upgrade

The main requirements for the Tracker Upgrade can be summarized as follows [1]:

1. Radiation tolerance The upgraded Tracker must be able to operate efficiently up to an integrated luminosity of 3000 fb^{-1}. The expected particle fluences that must be tolerated. This requirement must be fulfilled without any maintenance intervention for the Outer Tracker.

2. Increased granularity In order to ensure efficient tracking performance at high pileup, the channel occupancy must be maintained near or below the 1% level in all tracker regions, which requires higher channel density. An average of 140 collisions per bunch crossing is taken as the target number of pileup events to benchmark the performance of the detector.

3. Improved two-track separation The present Tracker has degraded track finding performance in high-energy jets, due to hit merging in the Pixel detector. In order to optimally exploit the statistics of the high-luminosity operation, the ability to distinguish two close-by tracks needs to be improved.

4. Reduced material in the tracking volume The performance of the current Tracker is significantly limited by the amount of material, which also affects the performance of the calorimeters and of the overall event reconstruction in CMS. Operation at high luminosity will greatly benefit from a tracker with significantly less material in the fiducial volume.

5. p_T distinction The upgraded Tracker should enable fast and efficient high

p_T distinction, which is particularly important for the high-level trigger (HLT).

In order to maintain or improve the physics performance of the CMS detector in the high pileup conditions of the HL-LHC, the entire tracking system must be replaced with new detectors featuring higher radiation tolerance and enhanced functionality. A sketch of one quadrant of the Phase-II Tracker layout is shown in Figure 1.4.

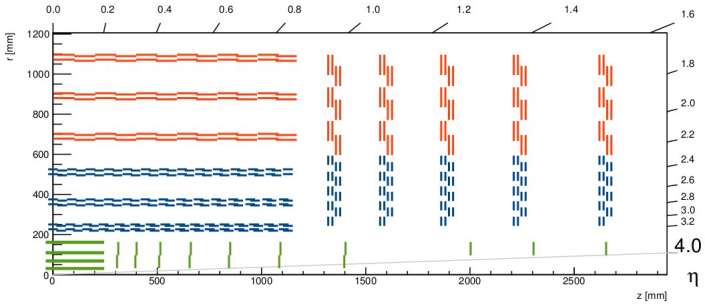

Figure 1.4: Sketch of one quarter of the new Tracker layout. Outer Tracker: blue lines correspond to PS modules, red lines to 2S modules. The Inner Pixel detector, with forward extension, is shown in green.

1.3 Silicon detectors

The CMS Tracker is completely made of silicon detectors, which are the best choice for tracking purposes in the LHC environment. Silicon has properties which make it especially desirable as a detector material.

- Small band gap E_g = 1.12 eV, E(e-h pair) = 3.6 eV ($\approx$ 30 eV for gas detectors), thus providing good signal.
- High specific density 2.33 g/cm^3 ; dE/dx (M.I.P.) $\equiv$ 390 eV/μm$\equiv$ 108 e-h/μm.
- High carrier mobility μ_e =1450 cm^2/Vs, μ_h = 450 cm^2/Vs, thus fast charge collection of less than 10 ns (better than gas detectors)
- Very pure, less than 1ppm impurities and less than 0.1ppb electrical active impurities, long mean free path, thus good charge collection efficiency.

- low dark current: Can be operated in air and at room temperature.
- low Z, thus low multiple scattering.
- Rigidity of silicon allows thin self supporting structures.
- Very well developed technology: microscopic structuring by industrial lithography
- Semiconductors provide high position resolution.
- They are radiation resistant.

For intrinsic silicon at room temperature (300 K) number of thermally created e^-h^+ pairs are four orders of magnitude larger than signal. Thus there is need to reduce free charge carriers, i.e. deplete the detector. Therefore the detectors make use of reverse biased p-n junction.

1.3.1 Principle of silicon detectors

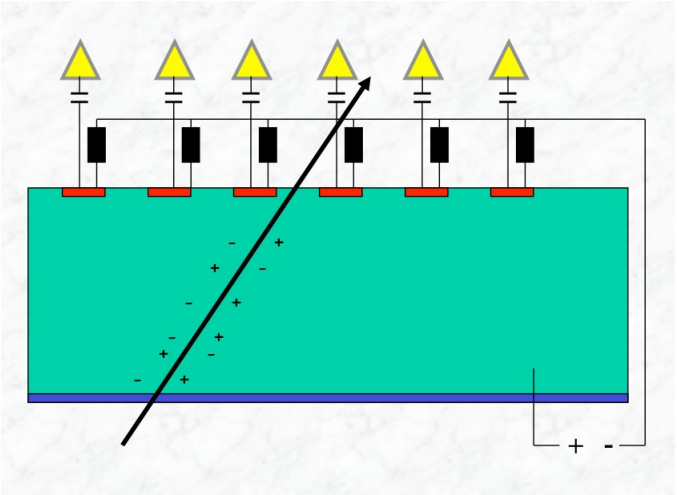

Figure 1.5: Schematic diagram of a MIP passing through a depleted p-n junction

e^-h^+ pairs are formed in the depletion region when a charged particle crosses the depletion region which drift towards the electrodes and give a small pulse. Cryogenic operation is required to mitigate leakage current.

Resolution σ depends on the pitch P (distance from strip to strip). For example detection of charge in binary way (threshold discrimination) and using

center of strip is measured coordinate results in $\sigma = P/\sqrt{12}$. Typical pitch values are 20 μm - 150 μm, e.g. 50 μm pitch results in 14.4 μm resolution.

1.4 Concept of p_T Module

The Outer Tracker provides data both for the L1 reconstruction (for each bunch crossing), and for the global event processing upon reception of a L1 trigger decision. The L1 functionality depends upon local data reduction in the front-end readout electronics, in order to reduce the required bandwidth of the L1 data stream. This is achieved with modules that are themselves capable of rejecting signals from particles below a certain transverse momentum (p_T) threshold, that are referred to as "p_T modules" [8].

The modules are composed of two closely spaced silicon sensors read out by a common front-end. The front-end ASICs correlate the signals collected in the two sensors, and select pairs that form "stubs" compatible with particles above the chosen p_T threshold. The strong magnetic field of CMS provides sufficient sensitivity to measure p_T over the small sensor separation, enabling the use of p_T modules in the entire radial range above $R \approx 20$cm. Stub data are sent out at every bunch crossing, while all other signals are stored in the front-end pipelines for reading out when a trigger is received. In order to implement the same p_T threshold for the stubs throughout the tracking volume, the acceptance window must be programmable in the front-end ASICs, and different sensor spacing must be implemented in different regions of the Tracker.

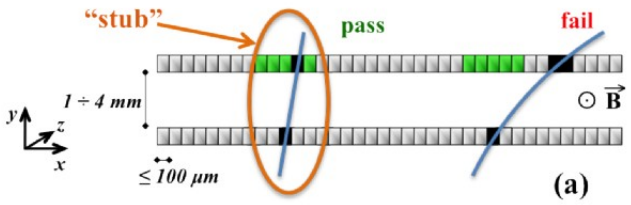

Figure 1.6: Correlation of signals in closely-spaced sensors enables rejection of low-p_T particles; the channels shown in light green represent the "selection window" to define an accepted "stub"

1.5 2S module

Two types of p_T modules are under development, the 2S module and the PS module. We are working on 2S module only which will be used for the outer tracker region. "2S" modules are composed of two superimposed strip sensors of approximately 10×10 cm^2 , mounted with the strips parallel to one another. They populate the outer regions, above $R \approx 60$ cm. The sensitive elements of the Outer Tracker are planar silicon sensors, which will be exposed to particle fluences up to $1.5 \times 10^{15} \eta_{eq}$ cm^{-2}, a factor of ten larger than the design requirement for the present Tracker.

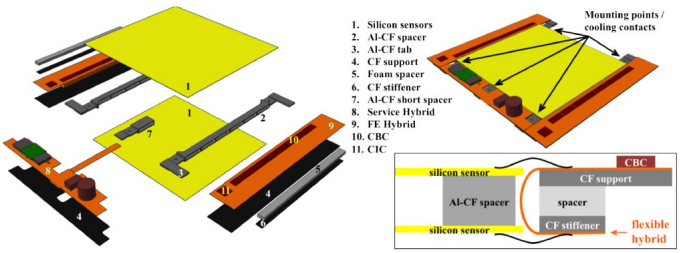

Figure 1.7: Exploded view of the 2S module components (left), 3D view of the assembled module (upper right), and a sketch of the FE Hybrid folded around its support (lower right).

Different types of substrates have to be utilized to achieve higher radiation tolerance. The choice of thin ($< 300\mu$m) sensors could offer advantages in terms of reduced leakage current and less material in the tracking volume. In addition, 300 μm sensors show higher CC than 200 μm sensors during annealing up to about 20 week. In order to achieve the required radiation tolerance it is critical to choose appropriate sensor material and processing technology. An extensive $R\&D$ program has been carried out to identify viable options and sensor designs for the Tracker and to define the requirements on the operating temperature. For the choice of the sensor polarity, the results collected thus far show that sensors with electron readout are more robust in terms of high-field effects after irradiation[9], and also provide higher CC than p-in-n sensors. Moreover, n-in-p sensors evade the higher complication and cost of production. The MCz material investigated shows lower full depletion voltages after irradiation compared to the FZ material.

Chapter 2

Beamtest

A few prototype detector modules have been constructed. In May 2016 BeamTest two 2S mini modules were tested

- Unirradiated module
- Module irradiated to a fluence of $6 \times 10^{14} n_{eq}/\text{cm}^2$

They were put under particle beam facility at CERN and we are studying their performance in detail. The properties that are being checked are mainly the efficiency to detect charged particle crossing the detector, the position measurement precision, the high p_T distinction of the modules, etc. The performance of ideal detector and irradiated detectors are also compared to understand the effect of the radiation damage..

2.1 Experimental Setup

The experimental setup is shown in Figure 2.1. The DUT (Detector under test) is the 2S mini module and the six telescope detectors (p0,p1,. . .,p5) are pixel detectors which are used for tracking. The Fe-I4 detector acts as trigger for the DUT. Once there is a hit on the Fe-I4 detector, it triggers the setup and the hits on each telescope detector and DUT at that time are recorded. The beam source is incident from the left of p0.

The module, as shown in Figure 2.2, has 2 sensors (dut0 and dut1) and each has 254 strips. The sensors have 2 CBC readout where each CBC reads out 254 channels, 127 from top sensor and 127 from bottom sensor.

The readout electronic system is fully digital and gives 1 if the signal is more than a threshold value, otherwise 0. Root tree files are generated from

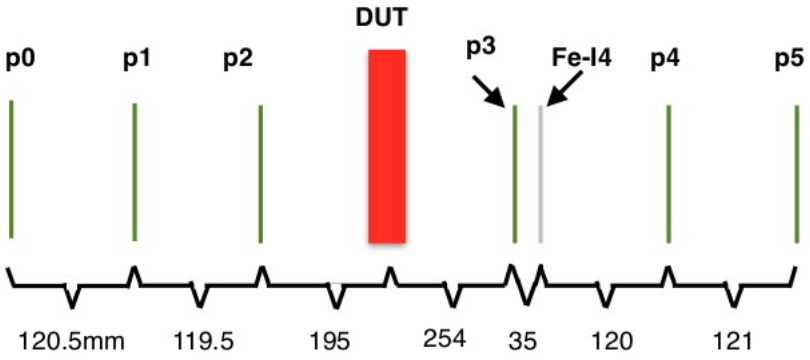

Figure 2.1: The schematic diagram of the experimental setup of the beamtest

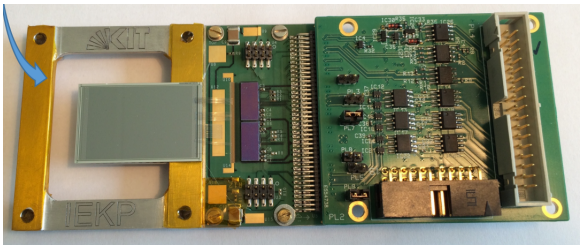

Figure 2.2: 2S mini module with CBC chip

signals from each channels, which represent a strip, which are then analyzed using C++ and Root[5] macro.

2.2 Analysis

Data is collected and stored in ROOT tree. When the signal on a strip is more than threshold voltage it is called **hit**. Hit on consecutive strips in the same sensor are called clusters and the number of strips in a cluster is called cluster width.

The beam profile on the unirradiated detector is shown in Figure 2.3. For an experimental run, the module was put under a low intensity beam and the number of events with hits vs strip number is plotted. The fiducial volume is defined as the volume of all working strips in the module.

The beam profile from strip number 1 to strip number 127 is obtained from CBC 0 and that from strip number 128 to strip number 254 is obtained from

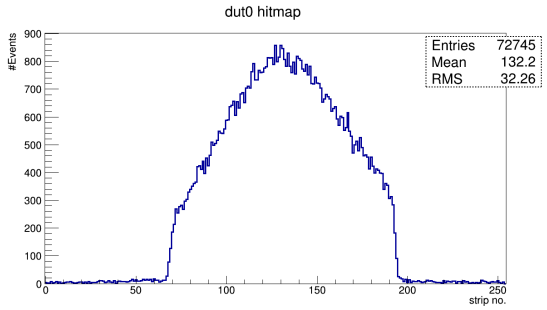

Figure 2.3: Beam profile as seen on the detector

CBC 1.

The cluster efficiency is defined as:

$$\text{Cluster efficiency} = \frac{\#\text{ events with atleast 1 matched cluster with 1 fid trk}}{\#\text{ events with 1 fiducial track}} \tag{2.1}$$

The position of a cluster can have 1 or 2 or multiple strips as shown in figure. For multi strip cluster we have a problem of defining the cluster position. By default cluster positions, given by the CBC, are integer value. For example, from Figure 2.4, where the shaded strips are the one with hits, for 2 strip cluster the cluster position is given as 4 and for 3 strip cluster the position is given as 9. During offline reconstruction, we introduce a floating value for the cluster position and it takes the cluster position for 2 strip cluster as 4.5, thus introducing a 1/2 strip correction. 1/2 strip correction can be observed in events with cluster width having even number of strips. The cluster efficiency with 1/2 strip correction is also compared with the default efficiency.

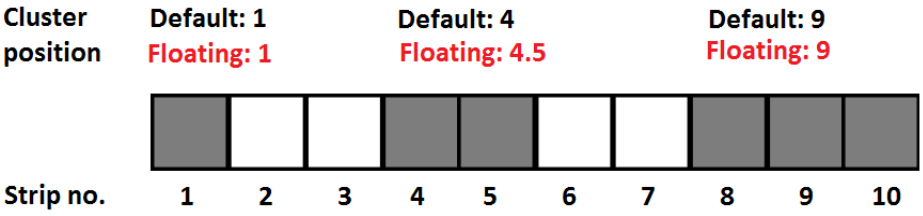

Figure 2.4: Cluster position for 1/2 strip correction

If clusters on the two sensors are correlated by the selection window then it

is called stub. The Stub efficiency is defined as:

$$\text{Stub efficiency} = \frac{\#\text{ events with atleast 1 matched reconstructed stub}}{\#\text{ events with 1 fiducial track}} \quad (2.2)$$

2.2.1 Cluster properties

Hits on consecutive strips is called **cluster**. Number of strips in a cluster is called **cluster width**. For a single run with VCTH 106 V and angle 0, the histogram of number of clusters and the cluster width is shown in Figure 2.5. It is observed that most of the events have 1 cluster (more than 95 %) and most of them have cluster width 1 ($\sim$ 90%). This is because the incident beam intensity was low.

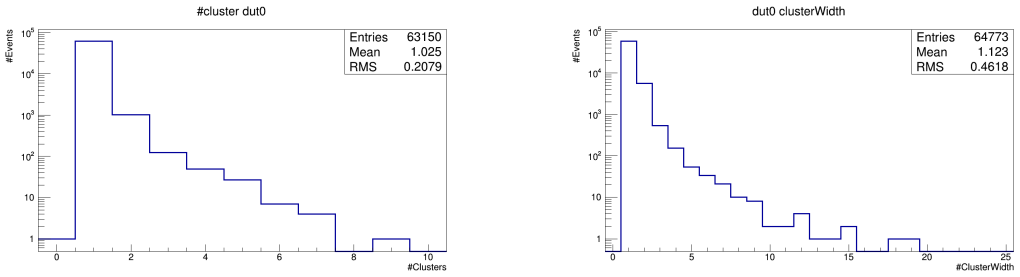

(a) Histogram of number of clusters

(b) Histogram of cluster width

Figure 2.5: Histograms of different cluster parameters for a run

2.2.2 VCTH Scan

In 2S module it has a digital electronics where a threshold is applied to separate the signal from the noise. Data are taken varying the threshold and to check the effect on the performance, namely hits, clusters and stubs. At higher negative threshold voltage it is expected that the signal will be dominant and at lower negative voltage noise will dominate. The stub constructing efficiency is investigated with the change of threshold. It is observed that due to large noise the stub efficiency is low at low negative threshold while at it is high due to strong signal at high negative threshold.

2.2.3 Angular Scan

The correlation window of the hits depend on the p_T of the track as well as the angle of incidence of the track. In CMS, due to the magnetic field, the trajectory of the particles bend according to their transverse momentum. In the beam test set up we have particle beams of a specific p_T. So the angle of the detector is varied and then try to verify the p_T-threshold of the detector. High angle corresponds to low p_T beam. It is observed that at a particular correlation window of 5, the stub efficiency of the module decreases with increasing angle, thus, with decreasing p_T.

The corresponding p_T scan is produced, using equation

$$p_T = 0.3 \times B \times \frac{r}{2 \times angle_{rad}} \tag{2.3}$$

where r is the radial distance of tracker from interaction point and B is the magnetic field. It is seen that there is a sharp change in stub efficiency at ~ 2 GeV.

The spacing between the top and bottom sensor for the unirradiated and irradiated modules are different, thus the p_T threshold for the two modules is different.

For the irradiated module, stub efficiency has been measured with different reverse bias voltage and has been optimized at 600 V. The reverse bias voltage for the irradiated module is high as high bias voltage is required to completely deplete the module after radiation damage and get high efficiency.

Angular Scan of cluster width mean is performed in Figure 2.6.

The mean increases as angle is increased, for both the sensors, because the

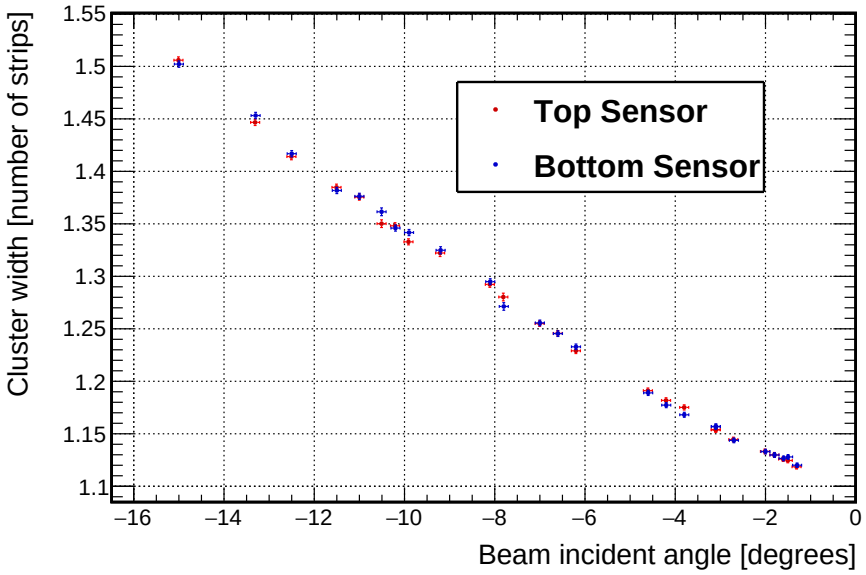

Figure 2.6: Cluster width vs angle for 2S unirradiated module

number of events with more than 1 cluster width increases. The cluster width for both the sensors is almost equal at all angles.

2.3 Results

2.3.1 Unirradiated Module

VCTH scan of cluster efficiency for each sensor of the unirradiated module is plotted.

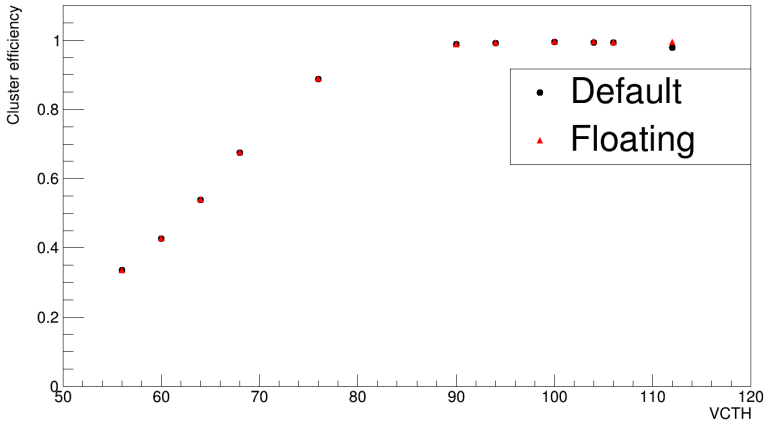

Figure 2.7: VCTH Scan of Cluster efficiency for sensor0 of unirradiated module

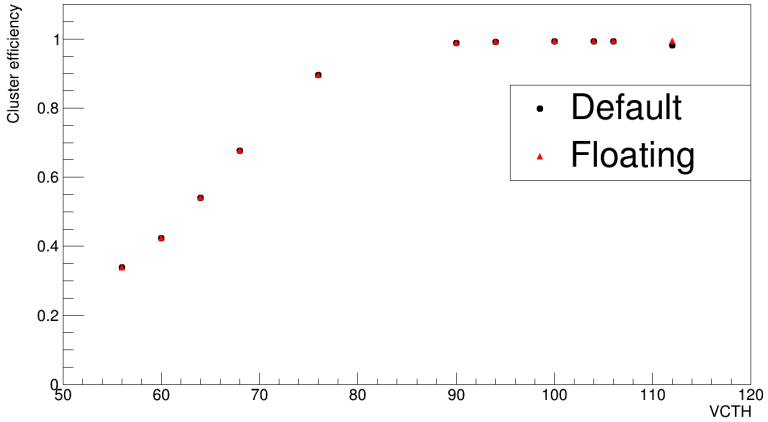

Figure 2.8: VCTH Scan of Cluster efficiency for sensor1 of unirradiated module

As the VCTH is increased, the number of matched clusters increases as the noise is suppressed, thus increasing the cluster efficiency of each sensor.

The VCTH scan of stub efficiency for the unirradiated module is shown in Figure 2.9.

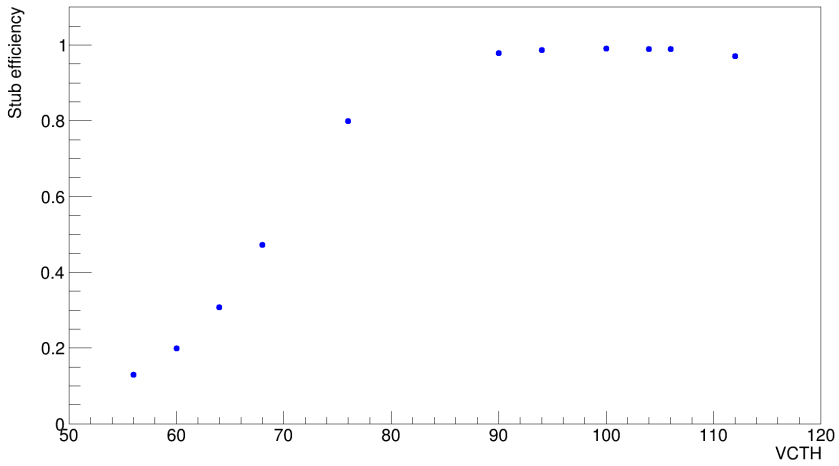

Figure 2.9: VCTH Scan of stub efficiency for unirradiated module

The stub efficiency of the module increases and saturates at high efficiency at VCTH value above 100 V. Thus, above 100 V the module is able to suppress the noise and yielding high efficiency.

Angular scan of cluster efficiency is plotted for each sensor of unirradiated module.

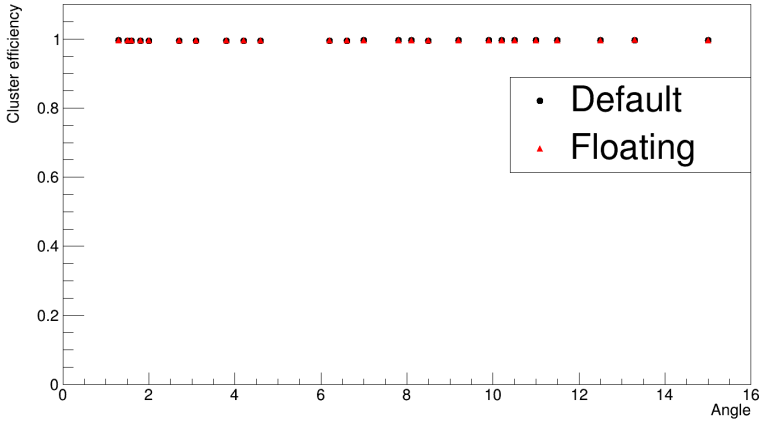

Figure 2.10: Angular Scan of Cluster efficiency for sensor0 of unirradiated module

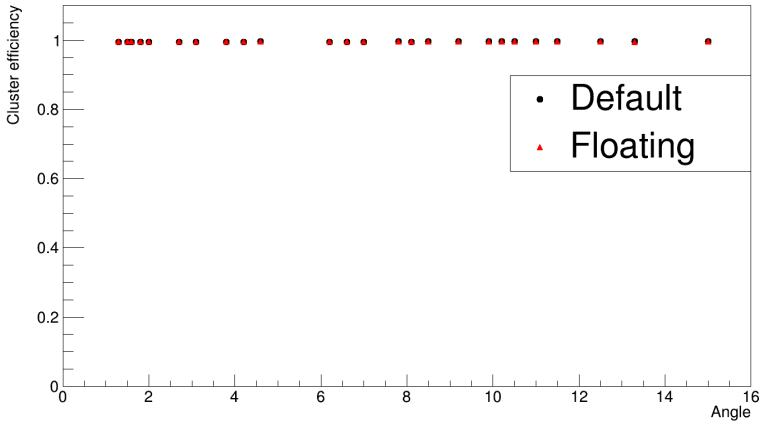

Figure 2.11: Angular Scan of Cluster efficiency for sensor1 of unirradiated module

The cluster efficiency remains constant with change of angle (or p_T) and no significant difference is observed in efficiency for the default and floating cluster positions.

The angular and corresponding p_T scan for unirradiated module to find the p_T threshold.

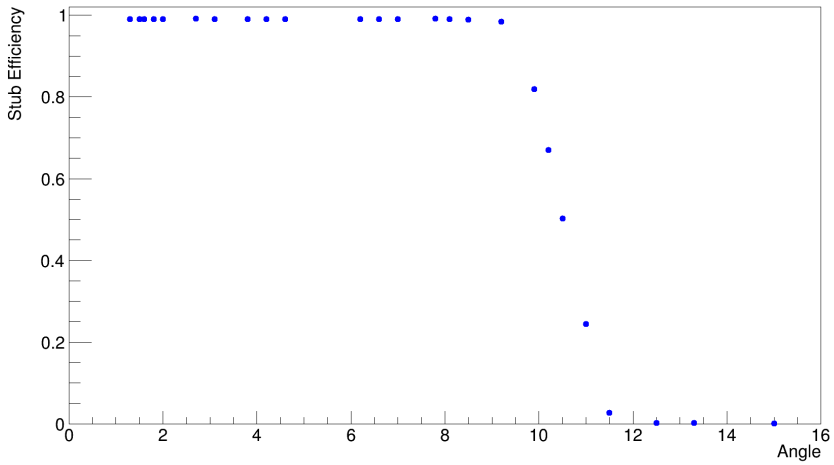

Figure 2.12: Angular Scan of stub efficiency for unirradiated module

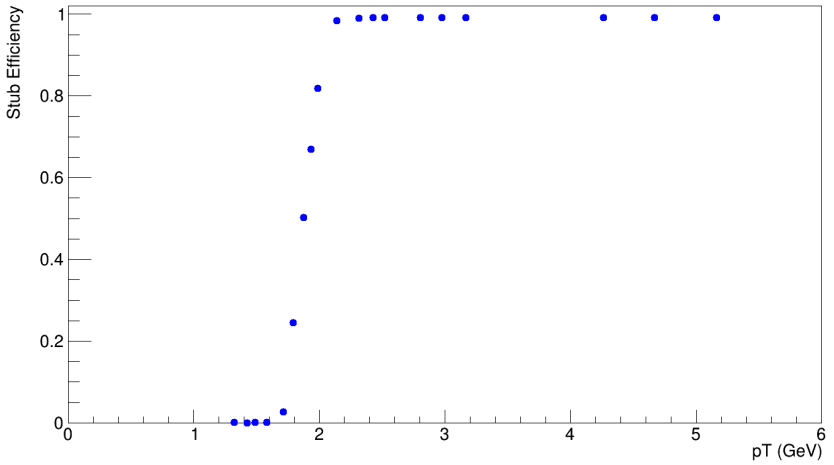

Figure 2.13: p_T Scan of stub efficiency for unirradiated module

The module is able to reject tracks below 2 GeV and give high efficiency above 2 GeV.

Stub efficiency for each strip in the unirradiated module is calculated with default and 1/2 strip corrected cluster position and compared.

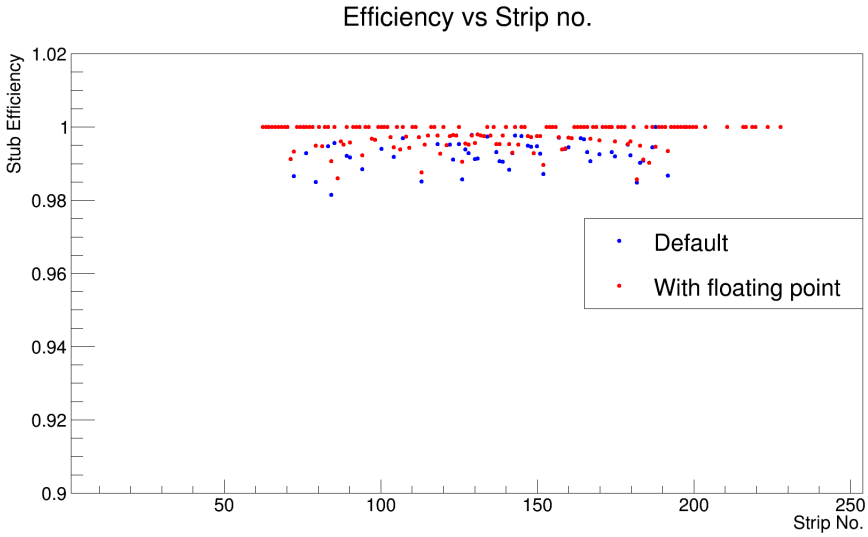

Figure 2.14: Strip stub efficiency for unirradiated module for an optimum run

Much difference in cluster efficiency, between default and floating cluster position value, is not observed in the modules and thus we look into the difference in each strip of the modules.

Stub efficiency values with the floating cluster position show significant improvements for some strips, thus highlighting the importance of the 1/2 strip correction.

2.3.2 Irradiated Module

The stub efficiency of the irradiated module is calculated with different bias voltage.

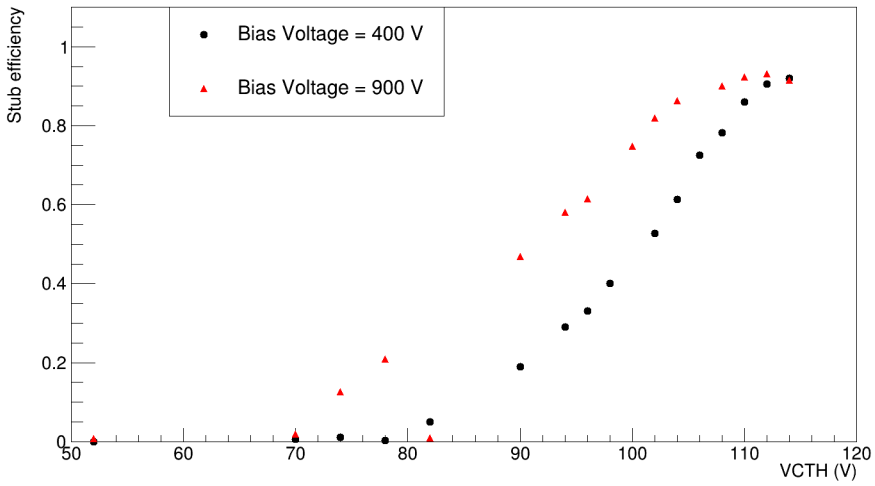

Figure 2.15: VCTH Scan of stub efficiency for irradiated module with different bias voltage

The efficiency is high and reaches the saturation at lower negative VCTH for high reverse bias voltage. Thus, the module is not fully depleted at 400 V and gives lower efficiency. High bias voltage is required to fully deplete the module.

The angular and corresponding p_T scan for the irradiated module at different bias voltage is done to find the optimum bias voltage.

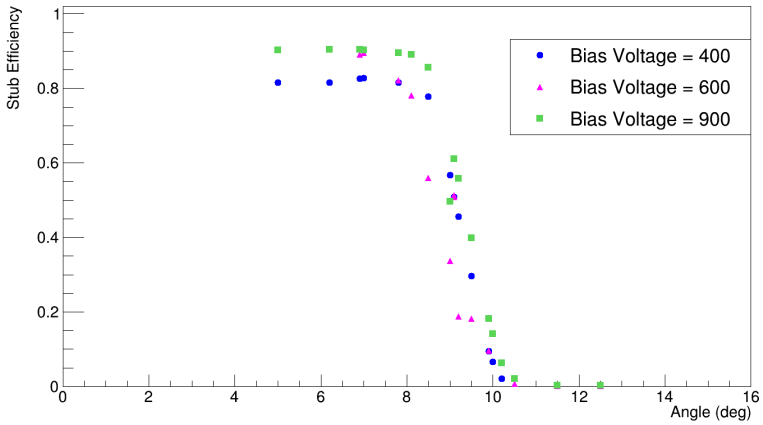

Figure 2.16: Angular Scan of stub efficiency for irradiated module with different bias voltage

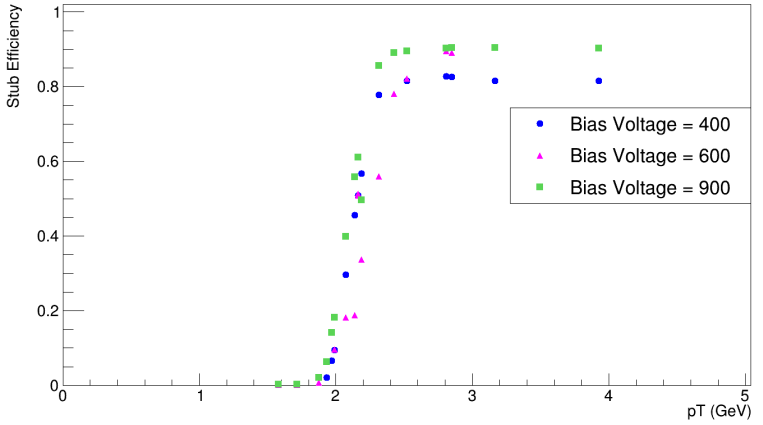

Figure 2.17: p_T Scan of stub efficiency for irradiated module with different bias voltage

From the above graphs it can be seen that the efficiency increases with increase in reverse bias voltage. This is because the module is more efficiently giving signals of tracks with increase of depletion region.

The angular and corresponding p_T scan with different selection window is done to observe the change in the p_T threshold.

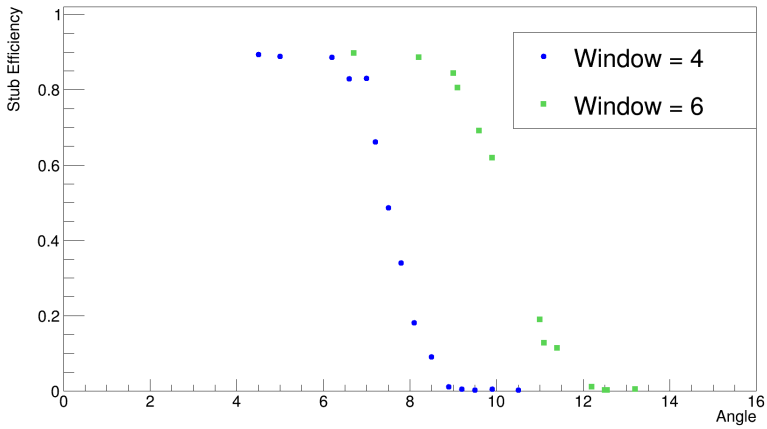

Figure 2.18: Angular Scan of stub efficiency for irradiated module with different selection window

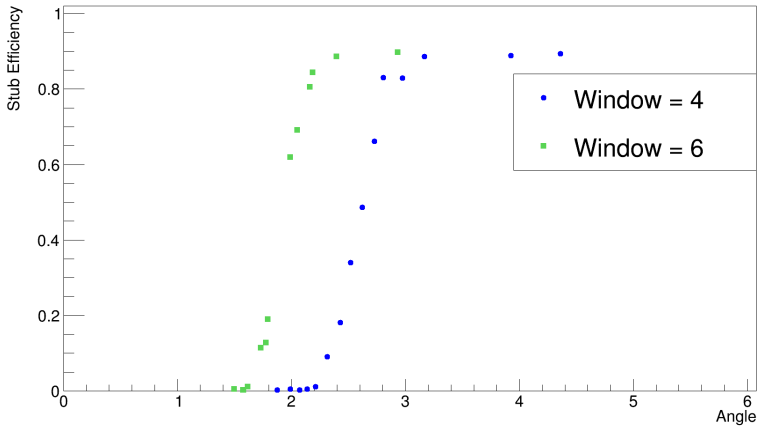

Figure 2.19: p_T Scan of stub efficiency for irradiated module with different selection window

Increasing the selection window results in the module selecting tracks with larger angle and thus reduced p_T. So, the p_T threshold is low for higher selection window.

Chapter 3

Summary and Conclusion

3.1 Summary

- CMS plans to upgrade its outer tracker with 2S modules and therefore new prototype modules are being tested ans studied. Efficiency and functionality of unirradiated and irradiated 2S module has been investigated.
- The module was designed to select tracks with p_T more than 2 GeV.
- The threshold scan was performed to find the optimum operating threshold of the sensors.
- The angular scan of stub efficiency and cluster width was performed. Results from cluster width scan will be used to tune the parameters of the simulation in the official CMS software.
- Using 1/2 strip correction we don't see any visible difference in the cluster efficiency of the sensors, but some improvements can be seen for stub efficiency of strips.
- The angular and threshold scan for irradiated module has been measured at different reverse bias voltages to optimize the bias voltage to get full depletion.

3.2 Conclusion

The present tracker modules need to be replaced as they cannot stand upto integrated luminosity of 3000 fb^{-1}. Also, at high luminosity, number of tracks will be very high and, thus, to eliminate storing uninteresting particle tracks, they should be able to distinguish particles above a certain p_T threshold. A threshold of 2 GeV corresponds to a data volume reduction of roughly one order of magnitude, which is sufficient for the purposes of L1 data transmission.

The module is able to identify p_T above a threshold ($\sim$2.4 GeV for unirradiated module and $\sim$2 GeV for irradiated module), depending on the separation between the sensors and the selection window, as the detector is efficiently able to select tracks with p_T above 2 GeV. Thus, the module can achieve the designed performance even after exposure to high fluence by increasing the reverse bias voltage and is suitable for Phase II upgrade.

The optimum working VCTH of the modules is found to be 110 V. The reverse bias voltage required to completely deplete the irradiated module and get maximum efficiency is 600 V. The cluster and stub efficiency measured from the cluster position given by CBC is almost equal to the offline 1/2 strip corrected efficiency and thus the CBC output is good enough for the purpose of CMS.

Appendix A

A.1 Glossary

- **CBC** CMS Binary Chip
- **cluster** hit on consecutive strips in the same sensor
- **cluster width** number of strips in a cluster
- **fiducial** the region of module with undamaged strips
- **hit** when the signal on a strip is more than threshold voltage
- **luminosity** luminosity is the ratio of the number of events detected in a certain time to the interaction cross-section
- **L1 trigger** Level 1 of the trigger is an extremely fast and wholly automatic process that looks for simple signs of interesting physics, e.g. particles with a large amount of energy or in unusual combinations.
- **pileup** average collisions per bunch crossing
- **PS** a p_T module with one layer of pixel sensors and another layer of strip sensors
  2S a p_T module with two layers of strip sensors
- **stub** if clusters in two sensors are correlated by a selection window
- **VCTH** threshold voltage of charge collected

A.2 Codes

Code for calculating efficiency

Code for plotting the efficiency

Appendix B

Bibliography

[1] CMS Collaboration, "Technical Proposal for the Phase-II Upgrade of the Compact Muon Solenoid", Technical Report CERN-LHCC-2015-010, LHCC-P-008, 2015.

[2] ATLAS Collaboration, "Observation of a new particle in the search for the Standard Model Higgs boson with the ATLAS detector at the LHC", Phys. Lett. B 716 (2012) 1, doi:10.1016/j.physletb.2012.08.020, arXiv:1207.7214.

[3] CMS Collaboration, "Observation of a new boson at a mass of 125 GeV with the CMS experiment at the LHC", Phys. Lett. B 716 (2012) 30, doi:10.1016/j.physletb.2012.08.021, arXiv:1207.7235.

[4] CMS Collaboration, "CMS Phase II Upgrade Scope Document", CERN-LHCC-2015-19 LHCC-G-165, 2015

[5] CMS Luminosity - Public Results (https://twiki.cern.ch/twiki/bin/view/CMSPublic/LumiPublicResults#Run_2_Annual_Charts_of_Luminosit)

[6] M. Moll, "Radiation Damage in Silicon Particle Detectors - Microscopic Defects and Macroscopic Properties".

[7] A. Ferrari, P. Sala, A. Fassò, and J. Ranft, "FLUKA: A multi-particle transport code (program version 2005)", Technical Report CMS-2005-010, 2005.

[8] C. C. Foudas, A. Rose, J. Jones, and G. Hall, "A Study for a Tracking Trigger at First Level for CMS at SLHC", arXiv:0510227.

[9] G. L. G.-L. Casse, A. A. Affolder, P. Allport, and M. Wormald, "Measurements of charge collection efficiency with microstrip detectors made on

various substrates after irradiations with neutrons and protons with different energies", in Proceedings of Science, PoS(VERTEX 2008), p. 036. 2008.